Liquid Structure, Infrared and Isotropic/Anisotropic Raman Noncoincidence of the Amide I Band, and Low-Wavenumber Vibrational Spectra of Liquid Formamide: Molecular Dynamics and ab Initio Molecular Orbital Studies

Hajime Torii* and Mitsuo Tasumi†

Department of Chemistry, School of Science, The University of Tokyo, Bunkyo-ku, Tokyo 113, Japan

Received: September 3, 1997; In Final Form: October 23, 1997[⊗]

The relationship between the liquid structure of formamide and wavenumber differences among its infrared (IR), isotropic Raman, and anisotropic Raman bands in the amide I region is analyzed theoretically. The following two methods are employed: (1) ab initio molecular orbital (MO) calculations on a few different cluster species of formamide molecules and (2) calculations of the IR and Raman spectra in the amide I region on the basis of the transition dipole coupling mechanism and the liquid structures derived from molecular dynamics simulations. It is shown that intermolecular interactions other than those involved in a one-dimensional hydrogen-bonded chain are required to reproduce the observed wavenumber difference between the amide I IR and isotropic Raman bands. This wavenumber difference originates from the difference in the vibrational patterns of the modes giving rise to these two bands. In the Raman noncoincidence, i.e., the wavenumber difference between the isotropic and anisotropic Raman bands, disorder in hydrogen-bonded chains in the liquid state plays an important role. Ab initio MO calculations of the low-wavenumber IR and Raman spectra of the cluster species of formamide are also performed. Existence of a large concentration of cyclic hexamers in the liquid state is unlikely because the low-wavenumber IR spectrum calculated for this cluster species does not account for the observed spectrum.

1. Introduction

Formamide is an amide compound with two hydrogen-bond donor sites in the molecule. Because of the existence of the NH hydrogen *cis* to the C═O group, the formamide molecule is capable of forming a cyclic dimer. Hydrogen bonding with the NH hydrogen *trans* to the C═O group gives rise to formation of a linear (zigzag) chain structure. A regular two-dimensional hydrogen-bond network in the crystalline state is constructed with these two types of hydrogen bonds.[1] In the liquid state, some of these hydrogen bonds are broken. As described below, a few different views on the liquid structure have been derived in the previous experimental and theoretical studies.

X-ray diffraction experiments on liquid formamide have indicated that this liquid mainly consists of linear hydrogen-bonded chains,[2] distorted cyclic dimer structures,[3] or both.[4] It has been suggested[5,6] that the strong bands observed in the low-wavenumber IR and Raman spectra (250−50 cm^{-1}) arise from linear hydrogen-bonded chains. However, since the features of the observed IR and Raman spectra of formamide in this wavenumber region are different from those of *N*-methylformamide and *N*-methylacetamide,[7−9] which are expected to form one-dimensional hydrogen-bonded chains in the liquid state, the origin of the observed spectral features should be examined in more detail. Comparisons between the observed and calculated results on the ^1H NMR chemical shifts, the ESCA spectra, and the dielectric constant have suggested[10] that a structure containing both linear zigzag chains and cyclic dimers is most likely for liquid formamide. Another study has suggested that the NMR spectra are consistent with the linear chain structure of liquid formamide.[11] A study on the Monte Carlo simulations of the liquid structure has supported this view.[12] However, the NMR quadrupole coupling parameters observed in a recent study[13] have been interpreted as indicating that liquid formamide is dominated by cyclic hexamer structures, which are formed by hydrogen bonding with the NH hydrogen *trans* to the C═O group.

Effects of intermolecular interactions can be seen not only in the low-wavenumber region but also in the amide I region (1750−1600 cm^{-1}). Mortensen et al.[14,15] have shown that the isotropic Raman band in the amide I region is significantly lower in wavenumber than both the IR and anisotropic Raman bands (with only a small wavenumber difference between the latter two). The wavenumber difference between the isotropic and anisotropic Raman bands is called the "Raman noncoincidence". In most cases, it is observed for a vibrational mode with a strong IR intensity[16−19] and is interpreted as arising from interactions between the transition dipoles of molecular vibrations in the liquid.[20,21] A coupling constant determined by the transition dipole coupling (TDC) mechanism[20,21] depends on the relative orientation of molecules involved in the coupling. It is therefore expected that information on the liquid structure, particularly the relative orientation of neighboring molecules, can be obtained by examining the vibrational spectra in the amide I region.

In the present work, the features of the IR and Raman spectra of formamide in the amide I region are analyzed theoretically with the following two methods: (1) ab initio molecular orbital (MO) calculations on a few different cluster species of formamide molecules and (2) calculations of the IR and Raman spectra

* Corresponding author. Telephone and facsimile: +81-3-3818-4621. E-mail: torii@chem.s.u-tokyo.ac.jp.

† Present address: Department of Chemistry, Faculty of Science, Saitama University, Urawa, Saitama 338, Japan.

⊗ Abstract published in *Advance ACS Abstracts,* December 15, 1997.

S1089-5647(97)02880-0 CCC: $15.00
Published on Web 01/01/1998

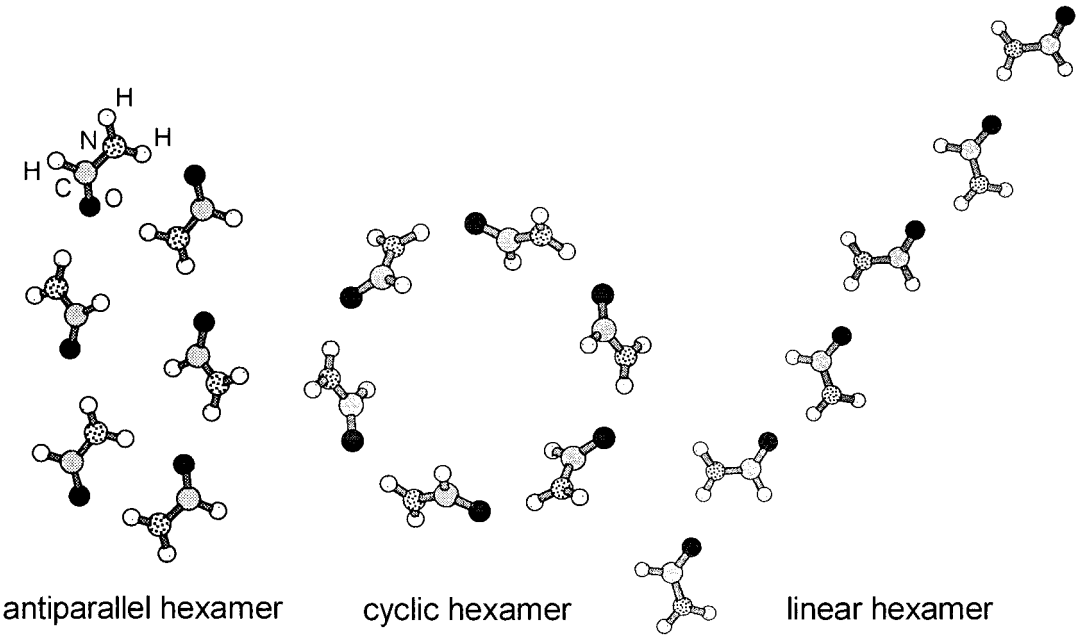

Figure 1. Structures of the cluster species treated in this study.

on the basis of the TDC mechanism and the liquid structures derived from molecular dynamics (MD) simulations. By using the first method, a structure−spectrum relationship is derived for a few ideal structures on the basis of the first-principle calculations. The low-wavenumber IR and Raman spectra calculated for the cluster species are also examined to support the results obtained from the spectra in the amide I region. In contrast, the effects of disorder in the liquid state on the spectra in the amide I region are analyzed by using the second method. Information on the liquid structure of formamide is obtained by these two complementary methods.

2. Computational Procedure

A. Ab Initio MO Calculations on Cluster Species. Ab initio MO calculations of IR and Raman spectra are carried out on the following cluster species of formamide: linear hexamer, cyclic hexamer, and a hexamer consisting of two antiparallel linear trimers that are hydrogen bonded with each other side by side (referred to as "antiparallel hexamer" hereafter). The structures of these cluster species are shown in Figure 1. The antiparallel hexamer can also be regarded as consisting of two cyclic dimers connected by two bridging molecules.

All the ab initio MO calculations are performed at the Hartree−Fock (HF) level. The 6-31G** basis set augmented by one set of diffuse functions on each of the oxygen and nitrogen atoms [denoted by 6-31(+)G** hereafter] is employed. The Gaussian 94 program[22] is used on IBM SP2 computers at the Computer Center of the Institute for Molecular Science and on a Hewlett-Packard workstation (Apollo 9000 series model 735) at the Research Centre for Spectrochemistry of the University of Tokyo.

At the HF/6-31(+)G** level, the formamide monomer has C_s symmetry at its potential energy minimum. In the minimum-energy structure of the antiparallel hexamer, the molecular planes of the bridging molecules are rotated to some extent from those of the other molecules, resulting in the C_i symmetry of this structure. At the potential energy minimum of the cyclic hexamer, the molecular planes are rotated alternately. This structure therefore has S_6 symmetry. By contrast, we assume C_s symmetry for the linear hexamer. This structure has one out-of-plane mode with an imaginary wavenumber. When an additional geometry optimization is performed along this mode (i.e., without any assumption about symmetry), we obtain the cyclic hexamer after many iteration steps. Since the cluster species treated in this study are intended to be models of structures in the liquid state, some of them may be different from the structures of isolated species at their potential energy minimum.

B. Calculations of Structures and Spectra of Liquid Formamide. MD simulations are performed on liquid formamide by using a polarizable intermolecular potential function derived by Gao et al.,[23] in which many-body interactions are taken into account by assuming isotropic polarizability on all the atoms. Intermolecular forces due to induced dipoles are calculated by the method described in ref 24. Only intermolecular degrees of freedom are considered. The molecular structural parameters are fixed to those given in ref 23. Four-dimensional vectors (quaternions) are used to represent molecular orientations in solving the equations of motion,[25,26] in combination with the leapfrog integration method.[26] The liquid system consists of 216 molecules in a cubic cell. The periodic boundary condition is employed. The volume of the cubic cell is fixed so that the molecular volume is equal to that given in ref 23. The temperature is kept at 298 K by adjusting the total kinetic energy every 200 fs. The time step is set to 2 fs. The system is equilibrated for 120 ps, after which a production run of 80 ps is carried out.

IR and Raman spectra are calculated by treating each molecule as an oscillator having a transition dipole, in the same way as in our previous studies.[21,27] This treatment is appropriate in the case where the vibrational band to be considered is sufficiently separated in wavenumber from other bands. Therefore, except for the discussion on the low-wavenumber spectra in section 3.C, we treat the case of formamide-d_2 ($HCOND_2$) in this study because the ND bending band is more separated from the amide I band than the NH bending band of the undeutrated species.

In the calculations of the IR and Raman spectra, liquid structures are extracted from the MD simulation (the production run of 80 ps) every 200 fs. The IR and Raman spectra

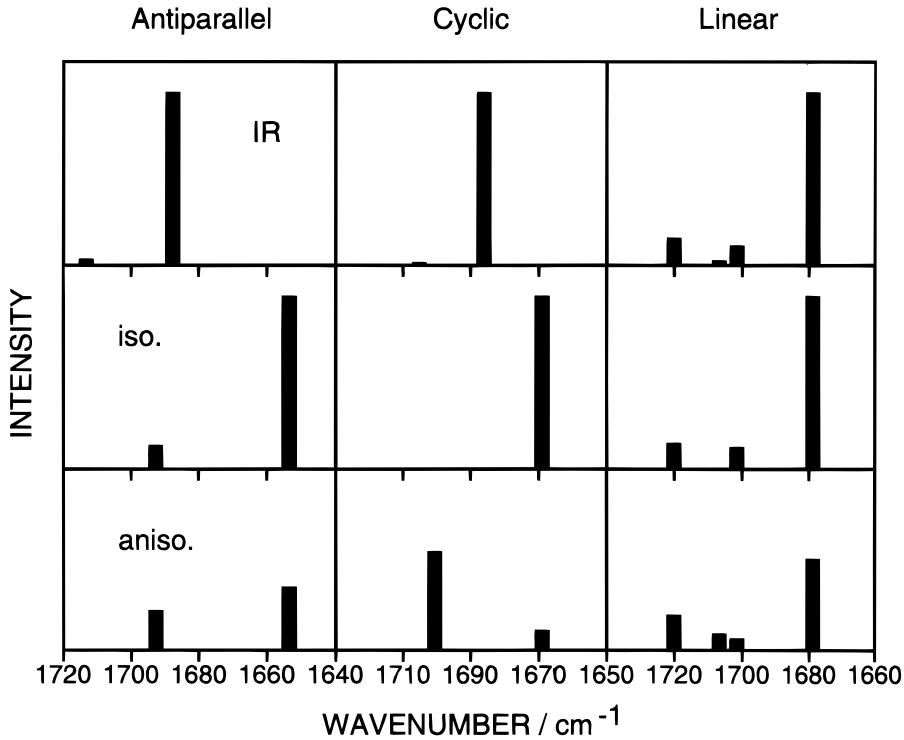

Figure 2. The IR, isotropic Raman, and anisotropic Raman spectra in the amide I region of the antiparallel, cyclic, and linear hexamers of formamide calculated at the HF/6-31(+)G** level.

calculated for such 400 instantaneous liquid structures are averaged. All the diagonal elements of the **F** matrix of the liquid system are assumed to be 1.651 mdyn $Å^{-1}$ amu^{-1}, which corresponds to an unperturbed vibrational wavenumber of 1674 cm^{-1}. The off-diagonal elements are determined by the TDC mechanism. The normal modes of the liquid system are calculated by diagonalizing the **F** matrix thus constructed. The transition dipole of the amide I mode, with a magnitude of 3.5 D $Å^{-1}$ $amu^{-1/2}$ and an angle of 20° from the C═O bond (tilted from the direction of O→C toward C→N), is assumed to be located at the center of the C═O bond, because the amide I mode mainly consists of the C═O stretch. The calculated spectra are not very sensitive to the location of the transition dipole. The direction of the transition dipole is consistent with the value of 15−22° calculated at the HF/6-31(+)G** level for the molecules in all the cluster species treated.[28] The magnitude of the transition dipole calculated at this level is in the range of 4.0−4.7 D $Å^{-1}$ $amu^{-1/2}$. The value adopted in this study (3.5 D $Å^{-1}$ $amu^{-1/2}$) is considered to be reasonable by taking into account that calculations at the HF/6-31(+)G** level tend to overestimate the values of vibrational transition dipoles. The Raman tensor of the amide I mode is assumed to be axially symmetric, with the principal axis tilted from the C═O bond by 60° (tilted from O→C toward C→N). From the results of the calculations on the cluster species at the HF/6-31(+)G** level, the principal axis of the Raman tensor tends to tilt from the C═O bond to a greater extent in a hydrogen-bonded molecule than in an isolated molecule. Wavenumber differences among the isotropic Raman, anisotropic Raman, and IR bands are not very sensitive to this tilt angle, although the calculated profile of the anisotropic Raman band slightly depends on it. Each calculated spectrum is convoluted with a Gaussian function with an appropriate width (half-width at half-maximum of 10 cm^{-1} for the isotropic Raman band and 20 cm^{-1} for the IR and anisotropic Raman bands) to take into account band broadening due to factors other than TDC. By this procedure, good agreement is obtained between the observed and calculated bandwidths, without affecting the first moments and the asymmetry of the band profiles.

The calculations described in this subsection are carried out on an NEC SX-3R supercomputer at the Computer Center of the Institute for Molecular Science.

3. Results and Discussion

A. Amide I Bands Calculated for the Cluster Species. The IR and Raman spectra in the amide I region of the antiparallel, cyclic, and linear hexamers of formamide-d_2 calculated at the HF/6-31(+)G** level are shown in Figure 2. The calculated wavenumbers are scaled uniformly by 0.89. There are six modes in total in this wavenumber region for each cluster species. However, some of them have negligible IR and Raman intensities and do not appear in this figure.

In the case of the linear hexamer, the lowest-wavenumber mode (1679 cm^{-1}) has the strongest IR and Raman intensities. All the molecules stretch in phase in this vibrational mode. Generally, such an in-phase stretching mode has a strong isotropic Raman intensity regardless of the structure of the cluster species. By contrast, the IR intensity of an in-phase stretching mode depends strongly on the relative orientation of molecules in the cluster. In the linear hexamer, all the C═O bonds are in the same direction. The vectors of transition dipoles of all the molecules are added with no cancellation for the in-phase stretching mode, resulting in a strong IR intensity, in the same way as in the in-phase amide I mode of the linear trimer of *N*-methylacetamide.[29] Therefore, as shown in Figure 2, no difference between the wavenumbers (1679 cm^{-1}) of the IR and isotropic Raman bands is seen for the linear hexamer. The calculated wavenumber of the anisotropic Raman band is also the same as that of the isotropic Raman band. This result is in contrast to the experimental result for liquid formamide, in which the isotropic Raman band is significantly lower in wavenumber than both the IR and anisotropic Raman bands (with only a small wavenumber difference between the latter

TABLE 1: Wavenumbers (First Moments, cm^{-1}) of the Infrared, Isotropic Raman, and Anisotropic Raman Components of the Amide I Band of Liquid Formamide

intermolecular interactions	ν_{IR}	ν_{iso}	ν_{aniso}	$\Delta\nu_{IR-iso}$	$\Delta\nu_{aniso-iso}$
calculated					
1 hydrogen bond, via *trans*-NH	1662.8	1657.0	1673.5	5.8	16.5
1 hydrogen bond, via *cis*-NH	1673.4	1668.1	1673.7	5.3	5.6
2 hydrogen bonds (cyclic dimer)	1674.3	1673.6	1673.6	0.7	0.0
all hydrogen-bonded pairs	1662.5	1650.6	1672.8	11.9	22.2
all non-hydrogen-bonded pairs	1682.8	1663.2	1675.2	19.6	12.0
within hydrogen-bond chains (*trans*-NH)	1663.3	1652.2	1673.6	11.1	21.4
all pairs	1671.4	1639.7	1674.0	31.7	34.3
observed[a]	~1670	~1640	~1675	~30	~35

[a] Reference 14.

two).[14,15] The spectral features observed for liquid formamide are not explained by the intermolecular interactions within a linear hydrogen-bonded chain.

In the case of the cyclic hexamer, the amide I modes belong to the a_g, e_u, e_g, and a_u symmetry species of the S_6 point group. As described above, the totally symmetric mode (a_g, 1669 cm^{-1}) has a strong isotropic Raman intensity. The doubly degenerate e_u modes (1686 cm^{-1}) have strong IR intensities. The a_u mode (1705 cm^{-1}) is also IR active, but its intensity is very weak. For a planar cyclic hexamer of C_{6h} symmetry (not shown), the corresponding mode is IR inactive (b_u). The doubly degenerate e_g modes (1701 cm^{-1}) are active only in the anisotropic Raman spectrum. Therefore, there are significant wavenumber differences among the IR, isotropic Raman, and anisotropic Raman bands calculated for this structure, in qualitative agreement with the experimental result for liquid formamide. However, the calculated wavenumber separation between the IR and anisotropic Raman bands is too large.

The calculated wavenumber difference between the IR and isotropic Raman bands is also significant for the antiparallel hexamer. In the strongly IR-active mode calculated at 1688 cm^{-1}, the C═O bonds in one hydrogen-bonded chain stretch, while the C═O bonds in the other hydorgen-bonded chain shrink. In the mode at 1654 cm^{-1} with a strong isotropic Raman intensity, all the C═O bonds stretch in phase. Interactions between the chains give rise to a large wavenumber separation between the IR and isotropic Raman bands. However, the wavenumber separation between the isotropic and anisotropic Raman bands observed in liquid formamide is not well reproduced by the calculation for the antiparallel hexamer, although the calculated intensity distribution is indeed different between the isotopic and anisotropic Raman spectra. The reason for this discrepancy is discussed below in section 3.B.

B. Amide I Bands Calculated for the Simulated Liquid Structures. The IR and Raman spectra in the amide I region calculated on the basis of the TDC mechanism and the liquid structures obtained from MD simulations are shown in Figure 3. The isotropic Raman band is calculated to be significantly lower in wavenumber than the IR and anisotropic Raman bands, in agreement with the experimental results.[14,15] The asymmetries in the observed band profiles are also reproduced qualitatively in the calculated spectra. The calculated wavenumbers (first moments) are shown on the row of "all pairs" (i.e., calculated by including interactions between *all pairs* of molecules) in Table 1. In ref 14, the observed IR band is decomposed into two components at ~1684 and ~1658 cm^{-1} because of the asymmetry of the band profile. The first moment of the observed IR band is therefore estimated to be about 1670 cm^{-1}. As shown in Table 1, the observed and calculated first moments are in reasonable agreement for each band.

To examine what kind of intermolecular interactions are

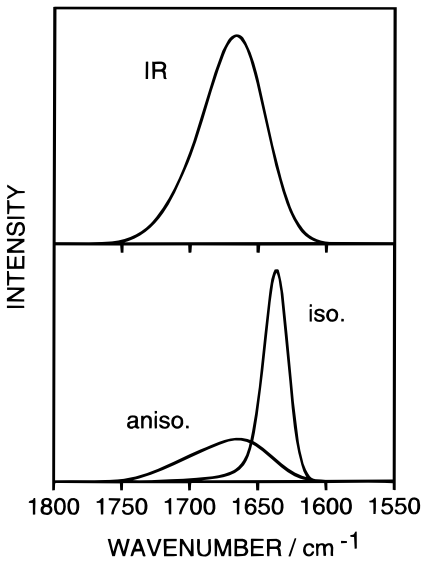

Figure 3. Calculated IR and Raman spectra in the amide I region of liquid formamide.

important for the wavenumber differences among the IR and Raman bands in the amide I region, $N(N-1)/2$ pairs of molecules (with N being the number of molecules in the system) are classified into a few categories, and vibrational wavenumbers are calculated by including only the vibrational coupling of the pairs belonging to a given category. In all cases, a common set of liquid structures derived from MD simulations are used. The results are shown in Table 1. A pair of molecules is regarded as hydrogen bonded if the O···H bond length is less than 2.6 Å and the C═O···H and O···H−N angles are both larger than 90°, on the basis of the O···H radial distribution function shown in ref 23. As shown on the first row in Table 1, the Raman noncoincidence ($\Delta\nu_{aniso-iso}$) arising from the vibrational coupling between molecules hydrogen bonded with the *trans*-NH hydrogen is noticeably large. However, the IR-iso wavenumber difference ($\Delta\nu_{IR-iso}$) arising from this type of coupling is small. The vibrational coupling between molecules interacting with the other types of hydrogen bonding has only small effects on both $\Delta\nu_{aniso-iso}$ and $\Delta\nu_{IR-iso}$ as shown in the second and third rows. In fact, there are a very small number of cyclic dimers in the simulated liquid structures. For both $\Delta\nu_{aniso-iso}$ and $\Delta\nu_{IR-iso}$, the value in the fourth row ("all hydrogen-bonded pairs") is nearly equal to the sum of the values in the first to third rows, indicating that the effects of the vibrational coupling on these values are almost additive. The interactions between hydrogen-bonded molecules explain about two-thirds of the value of $\Delta\nu_{aniso-iso}$ in the seventh row ("all pairs"), but only about one-third in the case of $\Delta\nu_{IR-iso}$. The difference between the values in the fourth and seventh rows is explained by the interactions of non-hydrogen-bonded pairs (the

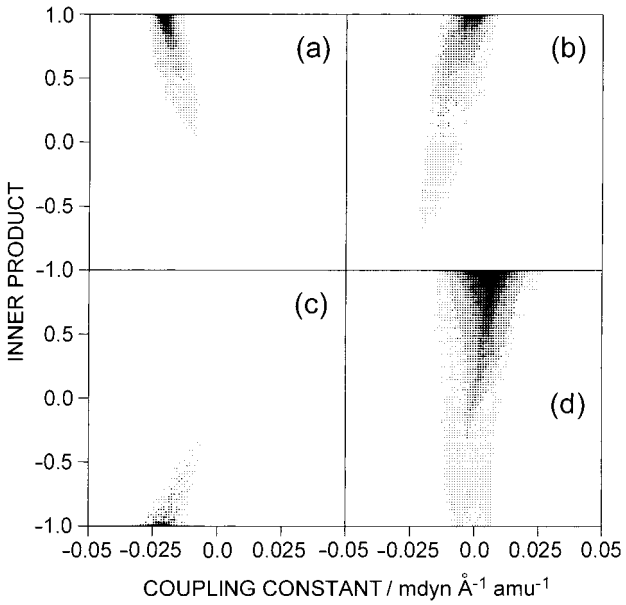

Figure 4. Correlation between the coupling constant and the relative orientation of (a) pairs of molecules bonded by one hydrogen bond to the *trans*-NH hydrogen, (b) pairs of molecules bonded by one hydrogen bond to the *cis*-NH hydrogen, (c) pairs of molecules with two hydrogen bonds in the cyclic dimer form, and (d) non-hydrogen-bonded pairs of molecules within 5.8 Å. The numbers of pairs are represented by dot sizes. The ratio of the number of pairs represented by the maximum dot size in each figure is (a):(b):(c):(d) = 20:8:1:20.

fifth row). The values in the sixth row include the effects of interactions between molecules that are not *directly* hydrogen bonded but are in a common hydrogen-bonded chain constructed by hydrogen bonds formed with the *trans*-NH hydrogens (e.g., between molecules A and C in a hydrogen-bonded chain of A−B−C). These values are similar to those in the fourth row rather than those in the first row. Since the value of $\Delta\nu_{\mathrm{IR-iso}}$ in the sixth row is significantly smaller than that in the seventh row, it may be said that interchain interactions by the TDC mechanism are important for this quantity.

The relation between a coupling constant and the relative orientation of molecules involved in the coupling is shown in Figure 4 for a few types of intermolecular hydrogen-bonding patterns. The relative orientation of molecules is represented by the inner product between the unit vectors along the transition dipole of the amide I mode. Parts a, b, and c of Figure 4 correspond to the first, second, and third rows in Table 1, respectively. Non-hydrogen-bonded pairs in the first solvation shell (i.e., within 5.8 Å) are included in Figure 4d. The numbers of pairs of molecules are represented by dot sizes, with a scale suitable for each figure as described in the caption.

As shown in Figure 4a, the inner product is positive and the coupling constant is negative for molecules hydrogen bonded with the *trans*-NH hydrogen. Due to the negative coupling constant, the in-phase amide I mode becomes lower in wavenumber than the out-of-phase mode. In this sense, the pairs of molecules classified into this category in the liquid are similar to those in the linear hexamer shown in Figure 1. However, deviation of the value of the inner product from unity is significant for some pairs because of the structural disorder in the liquid system. By comparing the results shown in Figure 2 (for the linear hexamer) and in Table 1 (for the liquid), it is considered that the large contribution of the molecules in Figure 4a to the calculated Raman noncoincidence (16.5 cm^{-1}) originates from the disorder in the hydrogen bonding to the *trans*-NH hydrogen in the liquid. It may be said that the large differences between ν_{IR} and ν_{aniso} calculated for the categories in the first and sixth rows in Table 1 are similar to that obtained for the cyclic hexamer in Figure 2. Indeed, molecules in the cyclic-hexamer form are included in these categories. However, no cyclic hexamer is found in the liquid structures derived from the MD simulations. Disorder in the structures of hydrogen-bonded chains may be more important than the closure of cyclic hydrogen bonds for the appearance of large Raman noncoincidence.

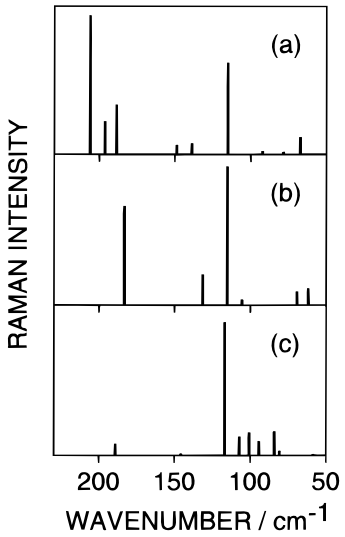

Figure 5. Calculated Raman spectra in the 230−50 cm^{-1} region of (a) the antiparallel hexamer, (b) the cyclic hexamer, and (c) the linear hexamer of formamide, in the $R(\nu)$ representation.

For the pairs of molecules bonded by one hydrogen bond formed with the *cis*-NH hydrogen shown in Figure 4b, the inner product is distributed over a wider range than the pairs in Figure 4a. The coupling constant is rather small, resulting in small contributions to the values of $\Delta\nu_{\mathrm{IR-iso}}$ and $\Delta\nu_{\mathrm{aniso-iso}}$ as shown in Table 1. The molecules in the cyclic dimer form (Figure 4c) have a negative inner product and a negative coupling constant. As a result, the Raman-active in-phase amide I mode is lower in wavenumber than the IR-active out-of-phase mode. However, because there is only a small number of pairs classified into this category in the liquid, the contribution to the values of $\Delta\nu_{\mathrm{IR-iso}}$ and $\Delta\nu_{\mathrm{aniso-iso}}$ is small. As shown in Figure 4d, the inner product is generally positive for the non-hydrogen-bonded pairs in the first solvation shell. However, a large number of pairs in the second solvation shell (not shown) have negative inner products. Although each coupling constant is small, the large number of pairs in this category gives rise to a significant contribution to the values of both $\Delta\nu_{\mathrm{IR-iso}}$ and $\Delta\nu_{\mathrm{aniso-iso}}$.

C. Vibrational Spectra in the Low-Wavenumber Region Calculated for the Cluster Species. The low-wavenumber Raman spectra calculated for the cluster species are shown in Figure 5. These spectra are presented in the so-called $R(\nu)$ representation,[6,8,9] which is calculated as $R(\nu) \propto I(\nu)\nu\,[1 - \exp(-h\nu/kT)] \propto A(\nu)\,[1 - \exp(-h\nu/kT)]$, where $I(\nu)$ stands for the Raman intensity in the usual sense and $A(\nu)$ is the Raman activity in units of Å^4 amu^{-1} calculated in the Gaussian program. The calculated wavenumbers in these spectra are unscaled.

In the observed Raman spectra of liquid formamide,[6] two broad and strong bands are observed at ∼200 and ∼100 cm^{-1}. The Raman spectrum calculated for the antiparallel hexamer shown in Figure 5a is consistent with this feature. In the Raman spectrum calculated for the cyclic hexamer shown in Figure 5b, the intensity of the mode at ∼180 cm^{-1} is slightly too weak

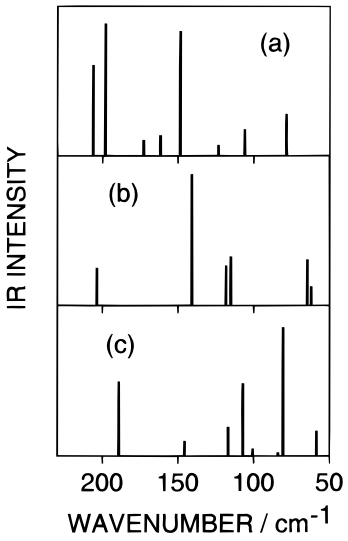

Figure 6. Calculated IR spectra in the 230−50 cm^{-1} region of (a) the antiparallel hexamer, (b) the cyclic hexamer, and (c) the linear hexamer of formamide.

compared with that of the mode at ∼100 cm^{-1}. For both of these cluster species, the depolarization ratios calculated for the modes giving rise to strong Raman intensities are equal or close to 0.75, in agreement with the experimental result.[6] By contrast, only one mode calculated at ∼115 cm^{-1} has a strong Raman intensity in the case of the linear hexamer shown in Figure 5c. Therefore, intermolecular interactions involved in a linear hydrogen-bonded chain (including a linear dimer treated in ref 30) are not sufficient to reproduce the feature of the observed Raman spectrum in the low-wavenumber region.

The low-wavenumber IR spectra calculated for the cluster species are shown in Figure 6. The calculated intensity patterns are significantly different among the three species. In the case of the antiparallel hexamer, two modes at ∼200 cm^{-1} and one at ∼150 cm^{-1} have strong IR intensities as shown in Figure 6a. In the IR spectrum of the cyclic hexamer, the intensity of the mode at ∼140 cm^{-1} is much stronger than those of the other modes, as shown in Figure 6b. For the linear hexamer, three modes with strong IR intensities are calculated at ∼190, ∼110, and ∼80 cm^{-1}, and the mode at ∼80 cm^{-1} has the strongest intensity.

In the observed IR spectrum of liquid formamide,[5] a broad and strong band is seen at ∼200 cm^{-1} with a tail extending to ∼100 cm^{-1}. A band with a medium intensity is seen at ∼150 cm^{-1} at lower temperatures,[5] although it is obscured in the liquid state at room temperature. This feature of the observed IR spectrum is well reproduced by the IR spectrum calculated for the antiparallel hexamer, but not by those for the other two species. Therefore, it may be said that there are a large number of hydrogen bonds formed with the *cis*-NH hydrogens. This result is consistent with the liquid structures derived from MD simulations.

The character of the low-wavenumber modes and the mechanism giving rise to the observed spectral features are discussed in detail elsewhere.[31] The Raman intensities in the low-wavenumber region are mainly determined by the rotation (libration) of the anisotropic polarizability tensor of each molecule, whereas the IR intensities in this region are determined by both the rotation (libration) of the permanent dipole moment of each molecule and the charge flux in the "cyclic dimer" parts in the system.[31] In such a case, the calculated IR and Raman intensities are considered to be sufficiently reliable.

4. Conclusion

The purpose of the present work is to study the relationship between the liquid structure and the features of the IR and Raman spectra of liquid formamide. Disorder in hydrogen-bonded chains is an important factor for the Raman noncoincidence ($\Delta\nu_{aniso-iso}$) in the amide I region. The intermolecular interactions within linear hydrogen-bonded chains explain about two-thirds of the observed value of $\Delta\nu_{aniso-iso}$. However, this is not the case for the value of $\Delta\nu_{IR-iso}$ in the amide I region, whether the disorder in the chain structure is taken into account. Interchain interactions by the TDC mechanism are important for explaining this quantity. The IR, isotropic Raman, and anisotropic Raman bands in the amide I region of liquid formamide originate from modes with different vibrational patterns. The vibrational coupling between molecules in the liquid gives rise to the difference in the wavenumbers of these bands.

The observed spectral features in the low-wavenumber region are well reproduced by the spectra of the antiparallel hexamer but not by those of the cyclic and linear hexamers. Therefore, it may be said that there are a large number of hydrogen bonds formed with the *cis*-NH hydrogens. It is considered that cyclic hexamers, which consist of hydrogen bonds formed only with the *trans*-NH hydrogens, are not dominant in liquid formamide.

References and Notes

(1) Ladell, J.; Post, B. *Acta Crystallogr.* **1954**, *7*, 559.
(2) Ohtaki, H.; Funaki, A.; Rode, B. M.; Reibnegger, G. J. *Bull. Chem. Soc. Jpn.* **1983**, *56*, 2116.
(3) Miyake, M.; Kaji, O.; Nakagawa, N.; Suzuki, T. *J. Chem. Soc., Faraday Trans. 2* **1985**, *81*, 277.
(4) Ohtaki, H.; Itoh, S. *Z. Naturforsch.* **1985**, *40a*, 1351.
(5) Itoh, K.; Shimanouchi, T. *J. Mol. Spectrosc.* **1972**, *42*, 86.
(6) Faurskov Nielsen, O.; Lund, P.-A.; Praestgaard, E. *J. Chem. Phys.* **1982**, *77*, 3878.
(7) Itoh, K.; Shimanouchi, T. *Biopolymers* **1967**, *5*, 921.
(8) Faurskov Nielsen, O.; Bigio, I. J.; Olsen, I.; Berquier, J.-M. *Chem. Phys. Lett.* **1986**, *132*, 502.
(9) Faurskov Nielsen, O.; Christensen, D. H.; Have Rasmussen, O. *J. Mol. Struct.* **1991**, *242*, 273.
(10) Pullman, A.; Berthod, H.; Giessner-Prettre, C.; Hinton, J. F.; Harpool, D. *J. Am. Chem. Soc.* **1978**, *100*, 3991.
(11) Hippler, M.; Hertz, H. G. *Z. Phys. Chem.* **1992**, *175*, 25.
(12) Jorgensen, W. L.; Swenson, C. J. *J. Am. Chem. Soc.* **1985**, *107*, 569.
(13) Ludwig, R.; Weinhold, F.; Farrar, T. C. *J. Chem. Phys.* **1995**, *102*, 5118.
(14) Mortensen, A.; Faurskov Nielsen, O.; Yarwood, J.; Shelley, V. *J. Phys. Chem.* **1994**, *98*, 5221.
(15) Mortensen, A.; Faurskov Nielsen, O.; Yarwood, J.; Shelley, V. *J. Phys. Chem.* **1995**, *99*, 4435.
(16) Fini, G.; Mirone, P. *J. Chem. Soc., Faraday Trans. 2* **1974**, *70*, 1776.
(17) Schindler, W.; Sharko, P. T.; Jonas, J. *J. Chem. Phys.* **1982**, *76*, 3493.
(18) Giorgini, M. G.; Fini, G.; Mirone, P. *J. Chem. Phys.* **1983**, *79*, 639.
(19) Zerda, T. W.; Thomas, H. D.; Bradley, M.; Jonas, J. *J. Chem. Phys.* **1987**, *86*, 3219.
(20) Logan, D. E. *Chem. Phys.* **1986**, *103*, 215.
(21) Torii, H.; Tasumi, M. *J. Chem. Phys.* **1993**, *99*, 8459.
(22) Frisch, M. J.; Trucks, G. W.; Schlegel, H. B.; Gill, P. M. W.; Johnson, B. G.; Robb, M. A.; Cheeseman, J. R.; Keith, T.; Petersson, G. A.; Montgomery, J. A.; Raghavachari, K.; Al-Laham, M. A.; Zakrzewski, V. G.; Ortiz, J. V.; Foresman, J. B.; Cioslowski, J.; Stefanov, B. B.; Nanayakkara, A.; Challacombe, M.; Peng, C. Y.; Ayala, P. Y.; Chen, W.; Wong, M. W.; Andres, J. L.; Replogle, E. S.; Gomperts, R.; Martin, R. L.; Fox, D. J.; Binkley, J. S.; Defrees, D. J.; Baker, J.; Stewart, J. J. P.; Head-Gordon, M.; Gonzalez, C.; Pople, J. A. *Gaussian 94*; Gaussian, Inc.: Pittsburgh, PA, 1995.
(23) Gao, J.; Pavelites, J. J.; Habibollazadeh, D. *J. Phys. Chem.* **1996**, *100*, 2689.

(24) Ahlström, P.; Wallqvist, A.; Engström, S.; Jönsson, B. *Mol. Phys.* **1989**, *68*, 563.
(25) Evans, D. J. *Mol. Phys.* **1977**, *34*, 317.
(26) Allen, M. P.; Tildesley, D. J. *Computer Simulation of Liquids*; Oxford University Press: Oxford, 1989.
(27) Torii, H.; Tasumi, M. *Bull. Chem. Soc. Jpn.* **1995**, *68*, 128.
(28) The transition dipole of each molecule in a cluster is calculated by dividing the eigenvectors of the (delocalized) amide I modes into elements of individual molecules and multiplying them by the dipole derivatives.
(29) Torii, H.; Tatsumi, T.; Kanazawa. T.; Tasumi, M. *J. Phys. Chem.* B **1998**, *102*, 309.
(30) Østergård, N.; Christiansen, P. L.; Faurskov Nielsen, O. *J. Mol. Struct.*: *THEOCHEM* **1991**, *235*, 423.
(31) Torii, H.; Tasumi, M. *Int. J. Quantum Chem.*, in press.